Behavior of Horizontal Shear Connections for Full-Depth Precast Concrete Bridge Decks on Prestressed I-Girders

Fatmir Menkulasi
Staff Engineer
Stroud, Pence and Associates
Virginia Beach, Virginia

Carin L. Roberts-Wollmann, Ph.D., P.E.
Assistant Professor
Virginia Polytechnic Institute and State University
Blacksburg, Virginia

This paper presents the results of a study of the horizontal shear resistance of the connection between full-depth precast concrete bridge deck panels and prestressed concrete girders. This connection consists of isolated shear connectors extending from the precast I-girder into a block-out pocket in the precast deck panel. The blockouts and the haunch between the panel and the beam are grouted. To investigate the strength and behavior of the connections, 36 push-off tests were performed. The primary parameters investigated were type of grout, haunch height, and area of reinforcing steel crossing the interface. In addition, several alternate shear connector details were tested. It was concluded that of currently known horizontal shear resistance equations, the one presented in the AASHTO LRFD Bridge Design Specifications is the best predictor of the strength of the specimens.

Bridge engineers and transportation agencies continually look for techniques to speed up construction of new bridges and replacement of deteriorated bridges. One concept for reducing construction time is the full-depth, full-width precast concrete bridge deck panel system. Fig. 1 illustrates the system supported on prestressed concrete I-girders.

The deck panels are full depth [7 to 9 in. (180 to 230 mm)], 6 to 10 ft (18 to 30 m) long in the direction of traffic, and full width of the bridge [up to 45 ft (14 m)] depending on transportation and handling restrictions. The decks are cast with pockets over the girders to accommodate the horizontal shear connectors.

After the new girders are erected or, in the case of a bridge deck replacement, the old deck is removed, the precast panels are set in position. The panels must be equipped with a leveling system over each girder to ensure that the panels are set to the proper elevation and that the dead load of each panel is well distributed to all girders. After the panels are in position, the panel-to-panel joints are filled with grout or epoxy, and longitudinal prestressing is applied. Finally, if horizontal shear connectors are post-installed, they are placed and the haunch, and

shear connector pockets are grouted after the shear connectors are installed.

After the grout has developed adequate strength and the guardrails have been placed, the driving surface is prepared, which may involve placing a sealer or overlay or grinding and grooving. After the surface is properly prepared, the bridge can be opened to traffic.

The system holds great promise for rapid bridge deck replacement. It could also become a low cost solution if the panels are standardized and the system is used widely enough that contractors become familiar with the construction process. The system is very durable because all the components are precast in a controlled environment, which alleviates early age deck cracking and differential and restrained shrinkage cracking. With prestressing in both directions, other types of cracking are also minimized or prevented.

The system should be improved with further refinement and testing. Simple and constructible details that account for construction tolerances and uncertainties are essential to rapid and trouble-free deck construction. Innovative approaches that would facilitate deck replacement require further investigation.

The research program described herein was an investigation of the horizontal shear capacity of full-depth precast panels on prestressed concrete I-girders. Three aspects of the horizontal shear transfer mechanism are quite different from typical cast-in-place decks on prestressed girders. These are:

1. There are two possible shear planes—one between the girder and haunch and the other between the haunch and deck panel.
2. The grout has no coarse aggregate, which affects aggregate interlock.
3. The connectors are clustered in isolated pockets.

To study the influence of these factors, a series of push-off tests were performed to quantify the strength of the joint. This paper presents the results of the push-off tests, compares the measured strengths to current code equations, and proposes alternate equations for nominal strength.

BACKGROUND

Considerable research into the design and behavior of precast deck panels on steel I-girders has been performed by Issa et al.[1-4] A full-depth panel system has also been developed and tested by Yamane et al.[5] A two-span continuous composite beam with precast deck panels was constructed and tested to failure by Chang and Shim.[6]

Horizontal shear connections for full-depth precast deck panels to steel I-girders was investigated by Shim et al.[7] They performed a series of push-off tests on a variety of shear stud connections placed in grouted pockets in precast concrete deck sections. The researchers investigated the influence of the type of bedding material and the depth of the haunch. They then calibrated finite element models to analyze the test results.

In previous research, the primary areas of investigation have been the

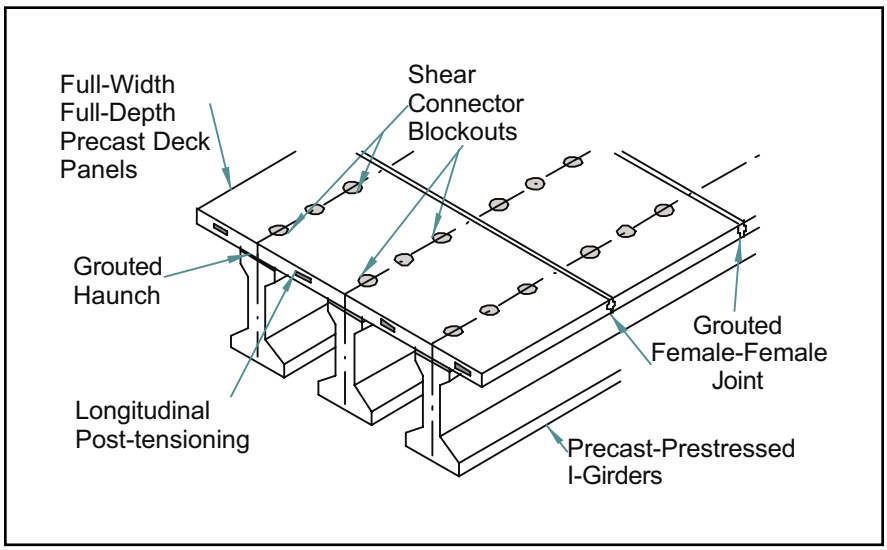

Fig. 1. Full-depth precast deck panel system.

Table 1. Equations for horizontal shear strength.

Code or specification	Horizontal shear strength
ACI 318-02	$V_u \le \phi V_{nh}$ No ties, clean, roughened surface: $V_{nh} = 80 b_v d$ (lbs) Minimum ties, clean, smooth surface: $V_{nh} = 80 b_v d$ (lbs) Ties provided, clean, roughened surface: $V_{nh} = [260 + 0.6 A_{vh} f_y/(b_v s)] b_v d$ not greater than $500 b_v d$ (lbs) If $V_u > \phi 500 b_v d$, design according to shear friction section Minimum ties: $A_{vh} = 0.75 \sqrt{f'_c}\, \frac{b_v s}{f_y}$ not less than $50 b_v s/f_y$
AASHTO Standard Specifications	$V_u \le \phi V_{nh}$ No ties, clean, roughened surface: $V_{nh} = 80 b_v d$ (lbs) Minimum ties, clean, roughened surface: $V_{nh} = 350 b_v d$ (lbs) Ties provided exceeding minimum, clean, roughened surface: $V_{nh} = 330 b_v d + 0.4 A_{vh} f_y d/s$ (lbs) Minimum ties: $A_{vh} = 50 b_v s/f_y$
AASHTO LRFD Specifications	$v_{uh} A_{cv} < \phi V_n$ $v_{uh} = V_u/b_v d_v$ $V_n = c A_{cv} + \mu (A_{vh} f_y + P_c)$ (lbs) where c = cohesion factor = 100 psi for clean and roughened surface μ = friction factor = 1.0 for clean and roughened surface P_c = permanent compressive force across interface

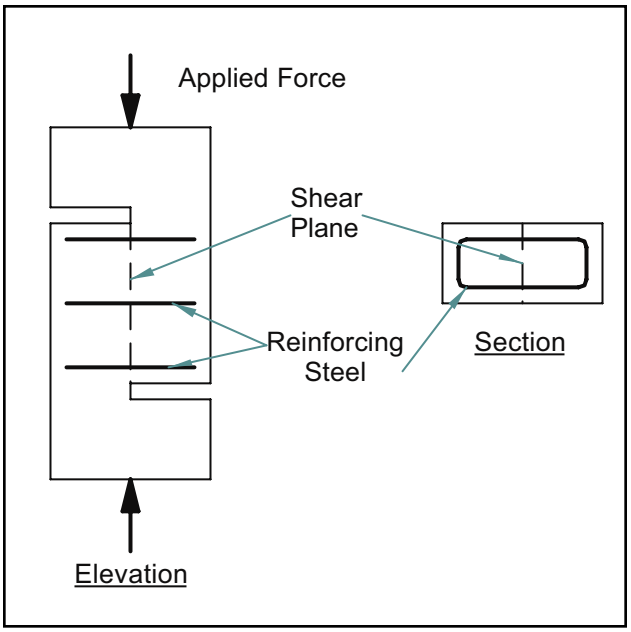

Fig. 2.
Typical push-off test configuration.

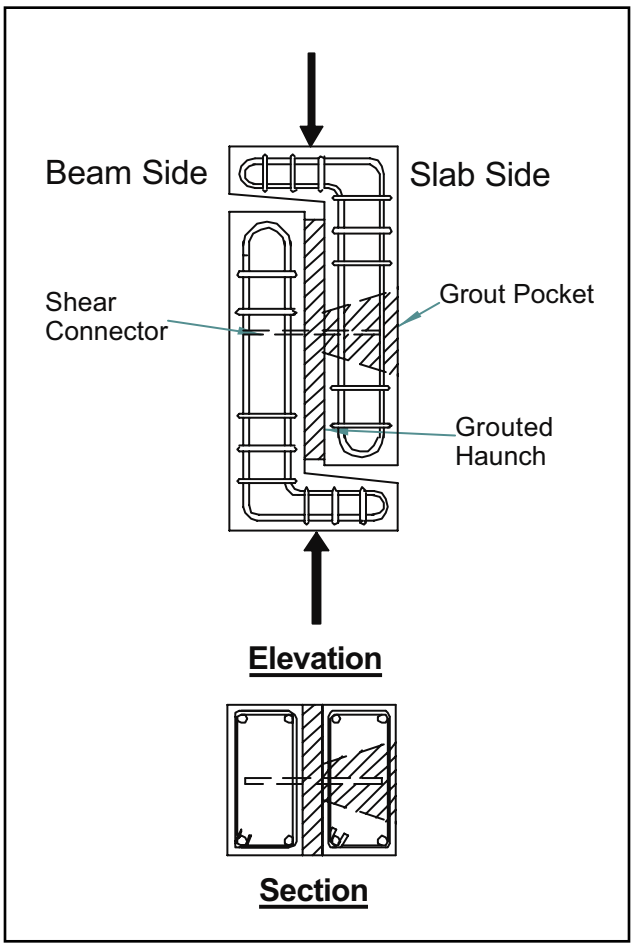

Fig 3.
Push-off test configuration for this investigation.

connections of the panels to the girders and the connections of the panels to each other. Much attention must be paid to these details to ensure that the decks are easily and quickly constructed, and further that they are durable and relatively maintenance-free. No known research to date has specifically addressed the connection of the panels to precast concrete girders.

Code and Specification Approaches

The ACI 318-02 Code,[8] the AASHTO Standard Specifications for Highway Bridges,[9] and the AASHTO LRFD Bridge Design Specifications[10] each have a slightly different approach to design for horizontal shear between a cast-in-place slab and a precast girder. Table 1 presents the methods of each of these codes of practice.

The formulation of each equation is basically the same. The shear that can be transferred across the interface, which is assumed to be new concrete cast against previously hardened concrete, can be quantified as a combination of cohesion and friction as follows:

$$V = C + \mu A_{vh} f_y \qquad (1)$$

where

C = cohesion (also encompasses dowel action and other contributing factors)

μ = friction coefficient

A_{vh} = area of reinforcing steel crossing the shear plane

f_y = yield strength of reinforcing steel

This formulation is typically referred to as a shear friction approach. The approach assumes that if a shear plane exists, such as a crack or an interface between concrete pours, as shear is applied and the two sections attempt to move relative to each other, a crack must open to allow for this movement. As the sections move relative to each other, if the cracked surface is rough, the two sections must ride up over that roughness, which will cause the crack to dilate. As the crack dilates, any reinforcement across the crack will be stressed and will most likely yield as the applied load is increased. This, in turn, will cause compression across the crack, and the shear resistance can be characterized by a friction coefficient times the compressive force.

Pioneering work in this area was performed by Mast,[11] Mattock et al.,[12-15] and Birkeland.[16] The typical type of test performed is known as a push-off test (see Fig. 2). The objective of this specimen shape and loading configuration is to apply a direct shear force, without any eccentricity at the interface. In this way the interface is tested only for its shear resistance. Several types of interfaces have been investigated, including uncracked monolithic normal-weight, lightweight and high strength concrete, monolithic precracked concrete, and new concrete poured against the old

concrete. Varying reinforcing steel ratios and normal compression and tension have been applied. But invariably, the results of the tests are quantified in terms of an equation similar to Eq. (1).

EXPERIMENTAL INVESTIGATION

The behavior and strength of the panel-to-supporting element connection, when the supporting element is a prestressed I-girder, was expected to be somewhat different from a typical composite girder interface (new concrete cast against old concrete) because of the presence of the grouted haunch, two interface planes, and isolated groups of connectors in grout pockets. This section presents the details of the testing program, which was performed to investigate the behavior and strength of this type of joint.

Push-off Tests

Thirty-six push-off tests were conducted, with the configuration of the specimens presented in Fig. 3. To represent the precast deck on a precast I-girder with a grouted haunch between, the specimens were cast as individual L-shaped specimens, one representing the beam with a protruding shear connector, and the other representing the precast slab with a blockout for the connector.

After the specimens were cured and removed from their forms, they were positioned adjacent to each other, with the shear connector extending into the blockout, and the space between, representing the haunch, and the pocket were grouted. When the grout reached the required strength, the specimens were loaded as shown in Fig. 3.

Specimen Details

Fig. 4 illustrates the details of the beam side specimen. The specimen is shown in the orientation in which it was cast. This orientation was selected so that the interface would mimic the top surface of a precast beam. At the time the concrete was placed, the top surface of each beam side specimen was raked to an amplitude of approximately ¼ in. (6 mm), as is typical for prestressed concrete beams.

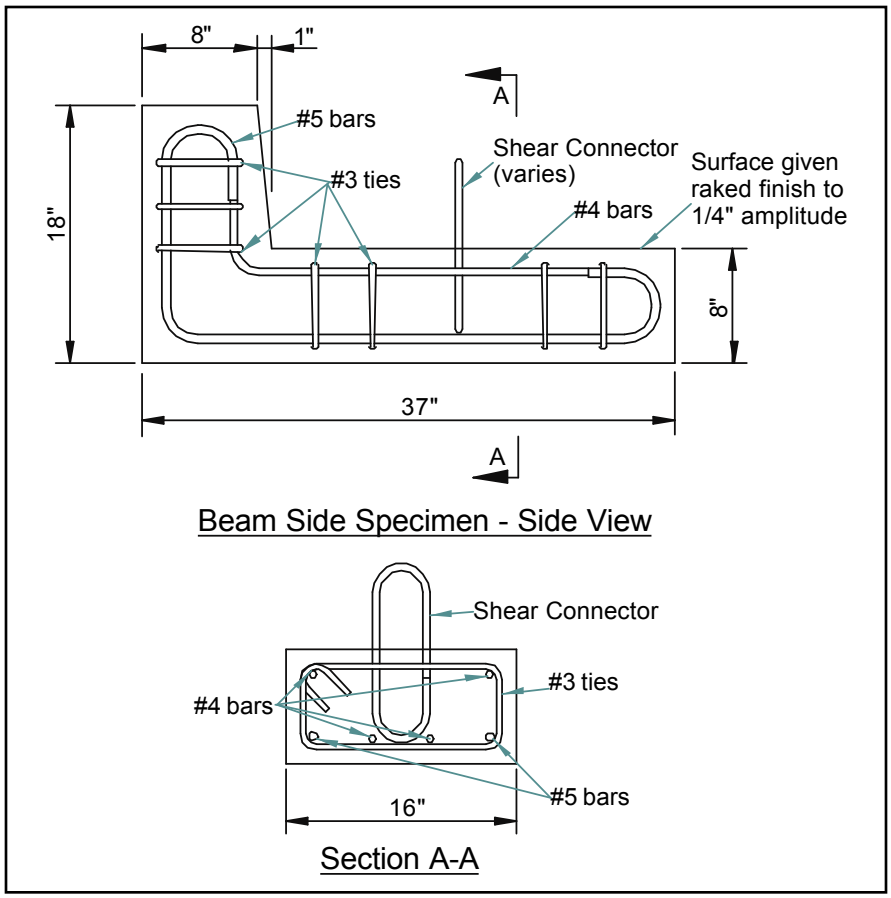

Fig. 4. Details of beam side specimen.

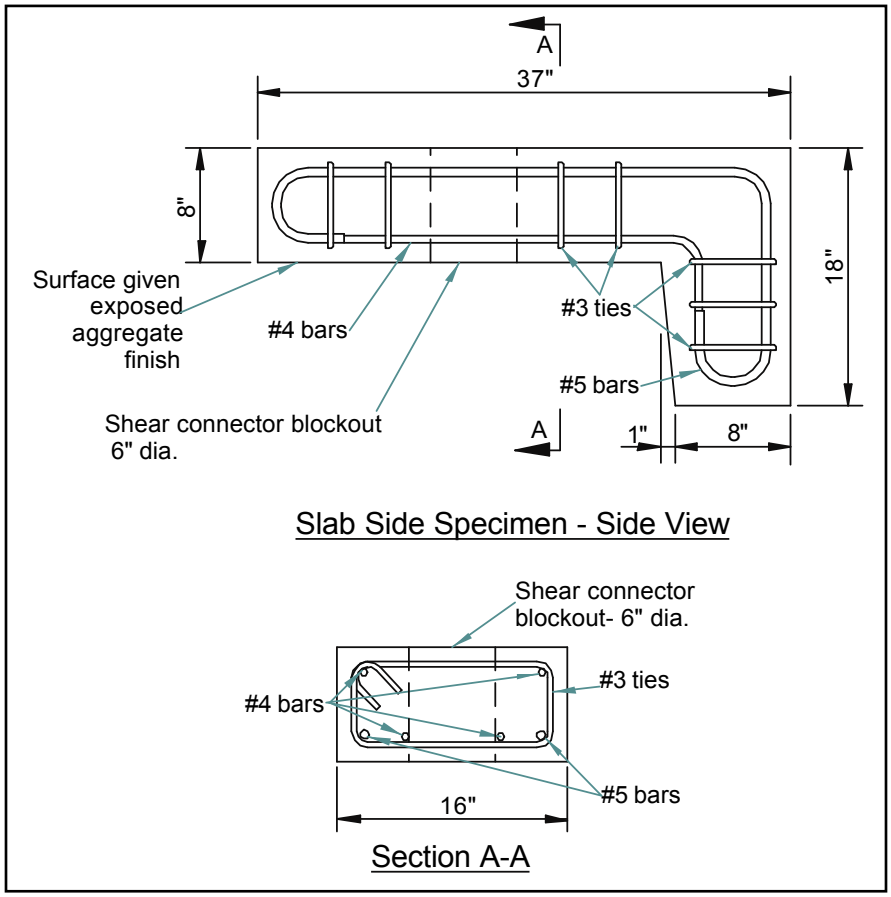

Fig. 5. Details of slab side specimen.

Fig. 5 illustrates the details of the slab side specimen. This specimen is also shown in the orientation in which it was cast. This orientation was selected to mimic the casting position of the slab, with the bottom surface on the formwork. To improve bond with the grouted haunch, a roughened surface was needed. Therefore, before placing the concrete, a retarder was placed on the formwork.

The day after placement, the slab formwork was stripped, and the bottom surface of the slab element was hosed with water to remove the outer sand and unhydrated mortar. This cleaning resulted in a rough, exposed aggregate finish.

The concrete used in the specimens was a nominal 4000 psi (28 MPa) mix with ¾ in. (19 mm) maximum aggregate size. The specimens were cast in three sets of 12 beam side and 12 slab side specimens. The actual concrete compressive strength at time of testing varied from 4200 to 5400 psi (29.0 to 37.2 MPa). The strength for each specimen is listed in Table 4.

After the specimens were cured and removed from their forms, they were positioned in pairs, and the space between the specimens, representing the haunch, and the blockout were grouted. Fig. 6 shows a typical specimen after grouting.

Two types of grout were evaluated: (1) a latex modified grout, and (2) a magnesium phosphate grout (Set 45, hot weather formulation, by Master Builders). For both types of grout, an angular pea gravel filler was added. Table 2 presents the mixture proportions for the latex modified grout.

The Set 45 grout was extended by adding 25 lb (11.3 kg) of angular ¼ in. (6 mm) aggregate to each 50 lb (22.7 kg) bag of Set 45. After the grout had attained the desired strength, a minimum of 3500 psi (24 MPa), the specimens were tested. The actual grout strength at the time of testing is listed in Table 4.

Fig. 6. Typical specimen with grouted haunch.

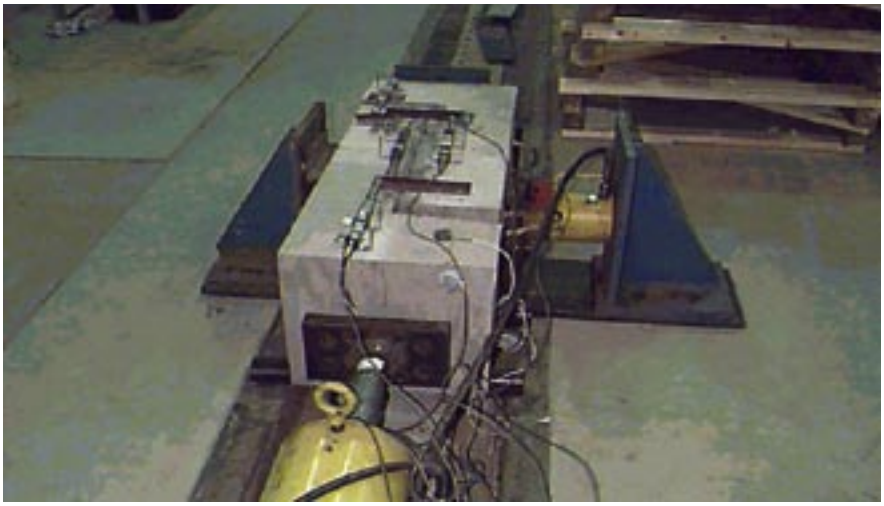

Fig. 7. Test setup for typical specimen.

Test Parameters

Several parameters were investigated in this testing program. These included (1) the type of shear connector, (2) the cross-sectional area of shear connector, (3) the type of grout, and (4) the haunch height.

The types of shear connectors included no connector, extended stirrups, post-installed reinforcing bars, and insert anchors. The three haunch heights investigated were 1, 2, and 3 in. (25, 51, and 76 mm). Table 3 presents the parameters of the 36 specimens. Typically, two repetitions of each set of parameters were performed.

Test Setup

After the interface grout had achieved the required strength, the specimens were prepared for testing. The assembled specimen was placed in a testing frame as shown in Fig. 7. The slab side of the specimen was fixed, and the beam side was able to slide relative to the slab side. The beam side was supported on four steel pipes, which served as rollers to allow the elements to slip relative to one another as the direct shear force was applied. The shear force was applied by a hydraulic ram and monitored by a 150 kip (670 kN) load cell.

A normal force was applied to represent the self-weight of the deck on top of the girder. A force of approximately 2.5 kips (11.1 kN) was calculated based on a 10 ft (3.1 m) girder spacing, an 8.5 in. (216 mm) thick deck, and a concrete unit weight of 150 lb per cu ft (2420 kg/m^3) over the 2 ft (610 mm) long interface. This force was applied to the slab side with a 10 kip (44 kN) ram and monitored with a 10 kip (44 kN) load cell. On the beam side, the normal force was resisted by an abutment, but the specimen was allowed to move in the direction of the applied shear force by a set of greased rollers.

Table 2. Latex modified grout mixture design.

Ingredient	Quantities per cu yd
Cement Type I/II	658 lb
Sand	1504 lb
Coarse aggregate	1250 lb
Water	146 lb
Latex	204 lb
w/c	0.38

Note: 1 cu yd = 0.76 m^3; 1 lb = 0.45 kg.

Instrumentation

The instrumentation that was used included the load cells, potentiometers to measure the slip at the interface, and bonded electrical resistance (ER) strain gauges to measure the strain in the shear connectors. The potentiometers can be seen in Fig. 7.

Test Procedure

The first operation in the test procedure was to apply the normal force on the slab element with a hydraulic ram. When the normal force reached approximately 2.5 kips (11.1 kN), the shear force was applied by the 150 kip (670 kN) ram. Load was increased until a crack formed. At this point, the specimen had a tendency to expand against the small ram, increasing the normal force. Before proceeding, the normal force was dropped back to 2.5 kips (11.1 kN). Loading continued until the specimens had slipped approximately 1 in. (25 mm).

TEST RESULTS AND ANALYSIS

This section presents results of the testing program. Typical plots of load versus slip are presented and failure modes discussed. All results are then compared to current code nominal strength equations. The load-slip and load-strain plots of all the tests can be found in Menkulasi's master's thesis.[17]

Load-Slip Behavior

Fig. 8 presents a comparison of the load-slip behavior of four specimens with varying amounts of horizontal shear reinforcement. All four tests had Set 45 grout and a 1 in. (25 mm)

Table 3. Test parameters.

Test number	Test designation	Type of grout	Haunch height, in.	Type of shear connectors	A_{vh}, sq in.
1 2	1H-0-LAT-A 1H-0-LAT-B	Latex	1	No connectors	0.0
3 4	1H-2#4-LAT-A 1H-2#4-LAT-B	Latex	1	1 No. 4 stirrup	0.40
5 6	1H-2#5-LAT-A 1H-2#5-LAT-B	Latex	1	1 No. 5 stirrup	0.62
7 8	1H-0-S45-A 1H-0-S45-B	Set 45	1	No connectors	0.0
9 10	1H-2#4-S45-A 1H-2#4-S45-B	Set 45	1	1 No. 4 stirrup	0.40
11 12	1H-2#5-S45-A 1H-2#5-S45-B	Set 45	1	1 No. 5 stirrup	0.62
13 14	3H-0-S45-A 3H-0-S45-B	Set 45	3	No connectors	0.0
15 16	3H-2#4-S45-A 3H-2#4-S45-B	Set 45	3	1 No. 4 stirrup	0.40
17 18 19 20	3H-2#5-S45-A 3H-2#5-S45-B 3H-2#5-S45-C* 3H-2#5-S45-D*	Set 45	3	1 No. 5 stirrup	0.62
21 22 23	1H-4#4-S45-A 1H-4#4-S45-B 1H-4#4-S45-C	Set 45	1	2 No. 4 stirrups	0.80
24 25	2H-2#5-S45-A 2H-2#5-S45-B	Set 45	2	1 No. 5 stirrup	0.62
26	3H-4#4-S45-A	Set 45	3	2 No. 4 stirrups	0.80
27 28	1H-2#5P-S45-A 1H-2#5P-S45-B	Set 45	1	2 hooked No. 5 bars post-installed	0.62
29	1H-2#6P-S45-A	Set 45	1	2 hooked No. 6 bars post-installed	0.88
30	1H-1#6P-S45-A	Set 45	1	1 hooked No. 6 bar post-installed	0.44
31 32	1H-4#5P-S45-A 1H-4#5P-S45-B	Set 45	1	4 hooked No. 5 bars post-installed	1.24
33 34	1H-0.75C-S45-A 1H-0.75C-S45-B	Set 45	1	¾ in. coil bolt	0.44
35 36	1H-0.75C-S45-SK-A 1H-0.75C-S45-SK-B	Set 45	1	¾ in. coil bolt	0.44

* C and D were performed because A and B had inadequate embedment of the stirrups into the deck.

Nomenclature:

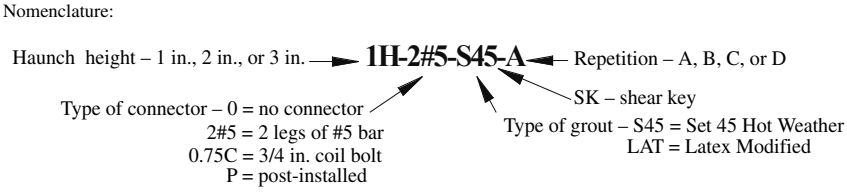

Table 4. Test results for Specimens 1 through 36.

Specimen number	Test designation	A_{vh}, sq in.	f_y, ksi	P_n, kips	s, in.	Clamp stress, psi*	f'_c, grout, psi	f'_c, concrete, psi	V_{peak}, kips	v_{peak}, psi	V_{sust}, kips	v_{sust}, psi
1	1H-0-LAT-A	0.0	—	2.5	26.5	6	6750	4200	94.9	224	8	19
2	1H-0-LAT-B	0.0	—	4.2	25.0	10	6750	4200	51.8	130	9	23
3	1H-2#4-LAT-A	0.40	64.8	4.1	26.5	71	6750	4200	63.4	150	27	64
4	1H-2#4-LAT-B	0.20	64.8	3.0	26.0	38	6750	4200	39.6	95	12	29
5	1H-2#5-LAT-A	0.62	66.1	2.8	26.5	103	6750	4200	69.9	165	37	87
6	1H-2#5-LAT-B	0.62	66.1	2.8	27.0	101	6750	4200	50.7	117	33	76
7	1H-0-S45-A	0.0	—	2.5	26.0	6	3600	4200	48.3	116	5	12
8	1H-0-S45-B	0.0	—	2.8	25.7	7	3600	4200	50.8	123	5	12
9	1H-2#4-S45-A	0.40	64.8	2.6	26.0	69	3600	4200	62.0	149	45	108
10	1H-2#4-S45-B	0.40	64.8	2.5	25.8	69	3600	4200	101.0	245	65	158
11	1H-2#5-S45-A	0.62	66.1	2.7	26.0	106	3600	4200	78.0	241	63	151
12	1H-2#5-S45-B	0.62	66.1	2.8	26.2	106	3600	4200	89.6	214	70	167
13	3H-0-S45-A	0.0	—	2.8	26.7	7	4380	5380	87.0	204	10	23
14	3H-0-S45-B	0.0	—	2.7	26.0	7	4380	5380	52.3	126	5	12
15	3H-2#4-S45-A	0.40	64.8	3.7	25.2	73	4380	5380	99.2	246	20	50
16	3H-2#4-S45-B	0.40	64.8	2.9	26.7	67	4380	5380	99.5	232	10	23
17	3H-2#5-S45-A	0.62	66.1	3.1	27.0	102	4380	5380	94.3	218	22	51
18	3H-2#5-S45-B	0.62	66.1	2.9	27.0	101	4380	5380	76.0	175		
19	3H-2#5-S45-C	0.62	66.1	2.8	25.8	106	3670	4800	92.8	225	63	153
20	3H-2#5-S45-D	0.62	66.1	2.7	25.5	107	3670	4800	104.2	255		
21	1H-4#4-S45-A	0.80	64.8	2.9	27.0	127	4380	5380	118.2	274		
22	1H-4#4-S45-B	0.80	64.8	2.8	26.3	130	4380	5380	115.7	275		
23	1H-4#4-S45-C	0.80	64.8	2.7	26.0	131	4380	5380	106.1	255	44	106
24	2H-2#5-S45-A	0.62	66.1	2.7	27.7	98	4380	5380	90.2	203	82	185
25	2H-2#5-S45-B	0.62	66.1	2.6	27.1	100	4380	5380	94.2	217	84	194
26	3H-4#4-S45-A	0.80	64.8	2.7	27.0	126	4380	5380	122.3	283	31	72
27	1H-2#5P-S45-A	0.62	66.1	2.5	26.3	213	3670	4800	83.3	198	58	138
28	1H-2#5P-S45-B	0.62	66.1	2.7	26.3	200	3670	4800	72.0	171	60	143
29	1H-2#6P-S45-A	0.88	66.1	2.9	26.5	144	3670	4800	73.0	172		
30	1H-1#6P-S45-A	0.44	66.1	2.6	27.0	73	3670	4800	106.1	246	38	88
31	1H-4#5P-S45-A	1.24	66.1	3.1	25.0	213	3670	4800	76.0	190		
32	1H-4#5P-S45-B	1.24	66.1	2.9	26.5	200	3670	4800	129.8	306	56	132
33	1H-0.75C-S45-A	0.88	100	2.7	26.5	214	3670	4800	117.6	277		
34	1H-0.75C-S45-B	0.88	100	2.7	25.5	222	3670	4800	90.4	222		
35	1H-0.75C-S45-SK-A	0.88	100	2.7	26.8	212	3670	4800	149.0	348	67	157
36	1H-0.75C-S45-SK-B	0.88	100	2.6	25.8	220	3670	4800	136.6	332		

*Clamping stress, $v_{clamp} = \dfrac{P_n + A_{vh} f_y}{b_v s}$

b_v = 16 in. for all specimens.

Note: 1 in. = 25.4 mm; 1 sq in. = 645 mm^2; 1 psi = 0.06895 MPa; 1 ksi = 6.895 MPa; 1 kip = 4.45 kN.

haunch, but the area of shear reinforcement varied. As seen in the plot, the peak load increased with increasing area of shear reinforcement. When the peak load was reached, a crack appeared along one of the interfaces. After cracking, the load was reduced, but typically the reduced load could be maintained through large slips.

In all tests, a crack opened at the interface between the grout and beam or slab element. In all tests with a 1 in. (25 mm) tall haunch, the crack occurred along the beam side. In specimens with a taller haunch, the location of the crack varied, and sometimes crossed through the haunch.

Load-Strain Behavior

Fig. 9 presents a typical load-strain plot for shear reinforcement. At the peak load, the strain in the reinforcing bars varied from test to test. In some of the tests, the strain prior to cracking of the interface was close to the yield strain, while in others it was much smaller. Once the specimen reached its maximum load and the crack formed, the strain in the reinforcing bar exceeded the yield point.

Of the 22 strain gauges that were applied and functioned, two indicated that the bar had yielded at the time of cracking. Both of these specimens had two No. 5 bars across the interface and showed evidence of earlier, more gradual interface slip. For both, the peak load was attained at a much larger slip than most specimens. For the remaining 20 gauges, the average strain at attainment of peak load was 760 microstrain, well below the yield strain.

Comparison of Grout Types

The primary goal of the first series of 12 specimens was to investigate the performance of the two different types of grout. For each type of grout, three horizontal shear connector details were tested: no connectors, two legs of No. 4 bar, and two legs of No. 5 bar.

Fig. 10 presents the peak shear stress of Tests 1 to 12 compared to the clamping stress. For this paper, these are defined as:

Clamping stress (psi):

$$v_{clamp} = \frac{A_{vh} f_y + P_n}{b_v s} \qquad (2)$$

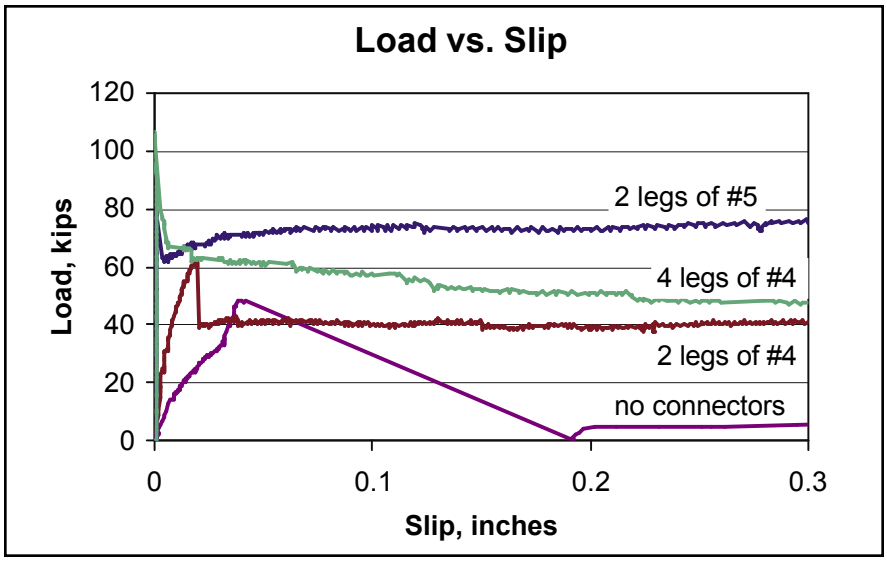

Fig. 8. Load-slip behavior of typical push-off tests.

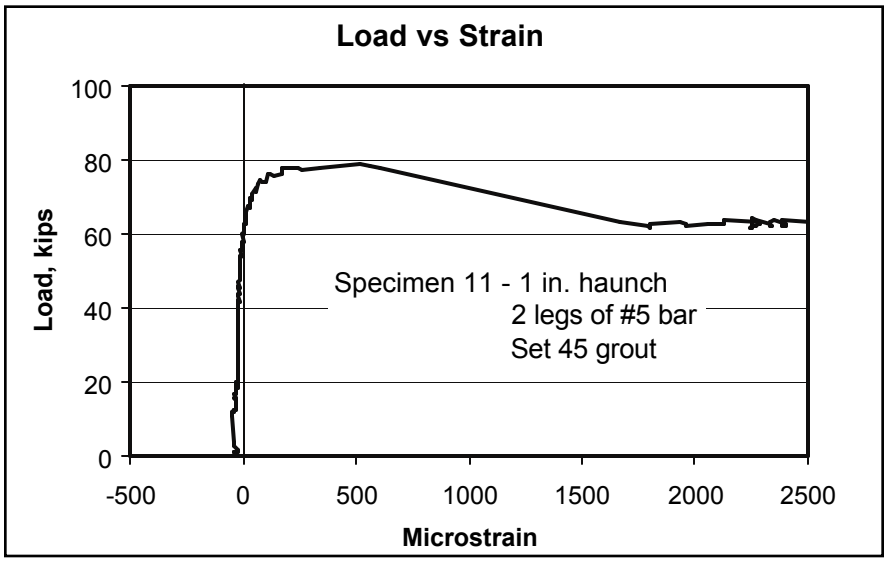

Fig. 9. Typical load-strain behavior of shear connector.

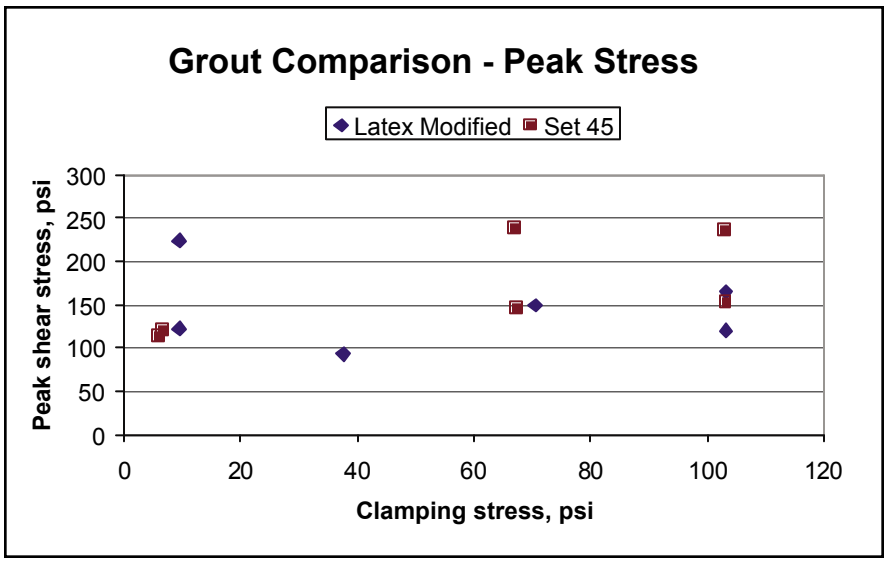

Fig. 10. Comparison of peak stresses for two grout types.

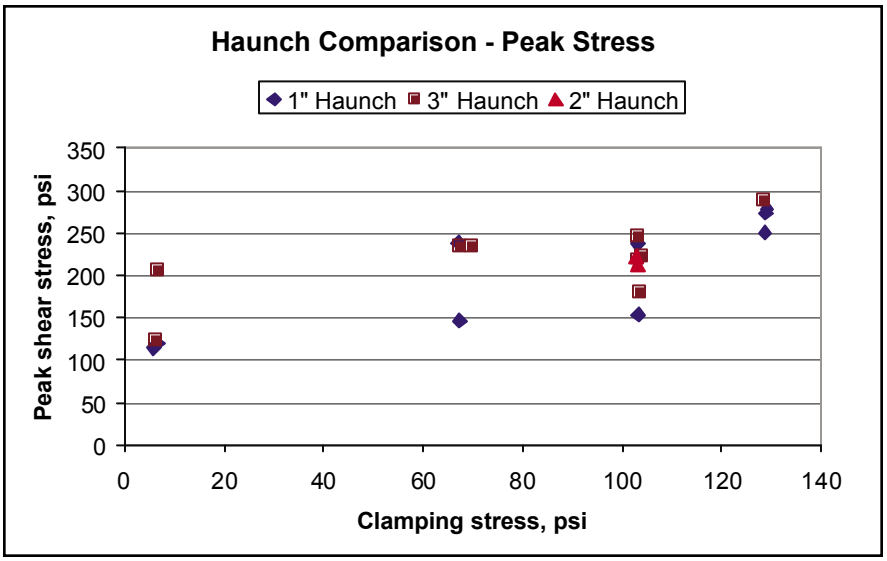

Fig. 11. Comparison of peak stresses for three haunch heights.

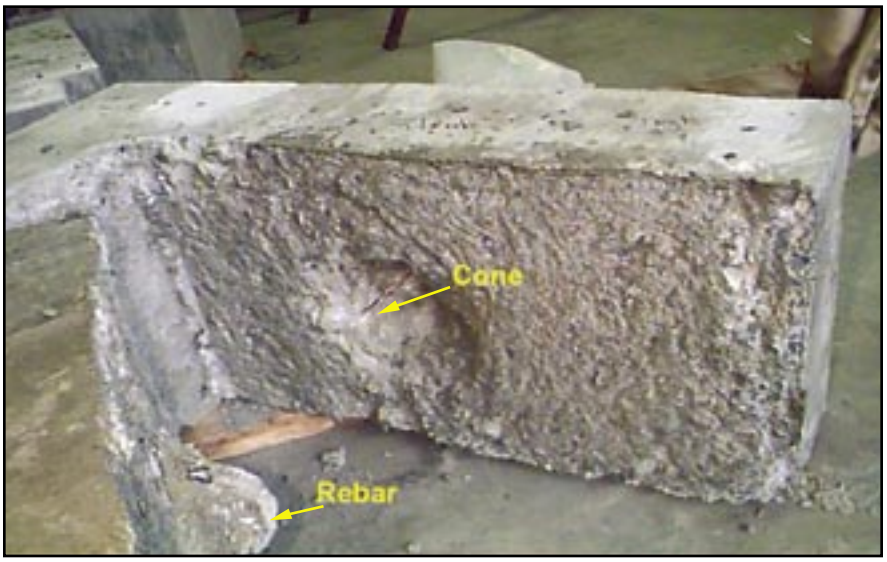

Fig. 12. Concrete cone break-out failure.

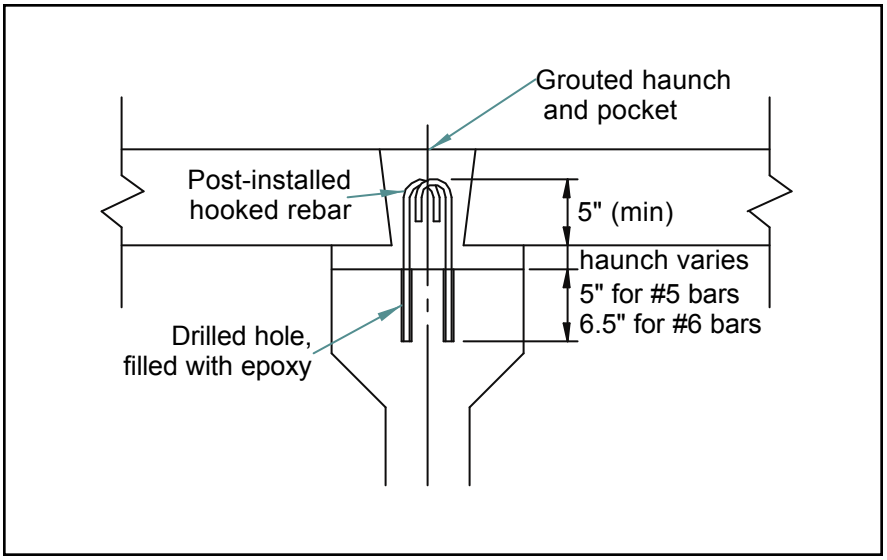

Fig. 13. Post-installed hooked reinforcing bar.

Peak shear stress (psi):

$$v_{peak} = \frac{V_{max}}{b_v s} \tag{3}$$

where

A_{vh} = area of reinforcing crossing interface, sq in.

f_y = yield stress of reinforcing steel, psi

P_n = normal force across interface, lbs

b_v = width of interface, in.

s = length of interface, in.

V_{max} = maximum applied shear force, lbs

The average peak shear stress for the Set 45 mix was 181 psi (1250 kPa), and the average peak shear stress for the latex modified mix was 147 psi (1010 kPa). Based on these results, the Set 45 mix was used in the remainder of the tests. It should be noted, however, that both types of grout exhibited considerable variability in the peak load for otherwise identical specimens.

Comparison of Haunch Heights

In a bridge, the haunch height will vary along the length of a beam because of the beam camber and the roadway geometry. The influence of the haunch height on the shear strength was investigated by testing several sets of specimens in which the area of steel reinforcement crossing the interface was the same, but the haunch height differed, either 1 or 3 in. (25 or 76 mm). For each haunch height, there were four connector details (no connectors, two legs of No. 4, two legs of No. 5 bar, and four legs of No. 4 bar). In addition, there was one detail (two legs of No. 5 bar) tested with a 1, 2, and 3 in. (25, 51 and 76 mm) haunch.

Fig. 11 presents the peak shear stress relative to the clamping stress for specimens with 1, 2 and 3 in. (25, 51, and 76 mm) haunch heights. As seen in the figure, there is no significant difference in strength associated with the changing haunch height. It should be noted, however, that the stirrups must have adequate embedment in the deck.

Note that due to an error in construction, one pair of specimens had the shear connectors extending only 3 in. (76 mm) into the deck side of the specimen. As a result, instead of a prolonged

post-peak load-slip behavior, the failure was more sudden and brittle.

The failure mode was a cone-breakout failure rather than a failure by yielding of the connector steel. The failure detail is shown in Fig. 12. Since the designer must ensure that the connectors extend an adequate distance into the pockets, which is at least 5 in. (127 mm) based on these tests, the extension of the connector out of the top of the precast beam may need to vary with the camber.

Alternate Shear Connectors

The goal of the last ten tests (Tests 27 to 36) was to investigate the performance of different types of shear connectors other than conventional extended stirrups. These shear connectors included post-installed hooked reinforcing bars and Dayton-Richmond anchors (see Figs. 13 and 14).

The hooked bars were very convenient and practical to install. After the concrete cured, a hole was drilled in the beam element. The hole was cleaned of dust by compressed air. Epoxy was then poured in the hole, and the hooked reinforcing bar was placed in the hole. The load-slip behavior of this type of anchor was quite similar to the cast-in-place reinforcing bars (see Fig. 15).

As can be seen in Fig. 14, the Dayton-Richmond anchors consist of two parts: the coil insert and the bolt. The coil insert is installed before the pouring of concrete on the beam element, and the bolt is threaded in once the beam and the slab element are placed together. One advantage of this type of shear connection is that during the construction process, there are no shear connectors extending from the tops of the girders.

Extended connectors can pose a tripping hazard and interfere with easy placement of the deck panels. Also, if future rehabilitation is required, the process of slab removal would be simplified because the bolts could be located, uncovered, and unscrewed.

Fig. 16 presents a typical load-slip plot for the specimens with the coil insert connection. As can be seen in the plot, both specimens maintained the post-peak load reasonably well.

Two tests investigated the use of shear keys on the beam side. These

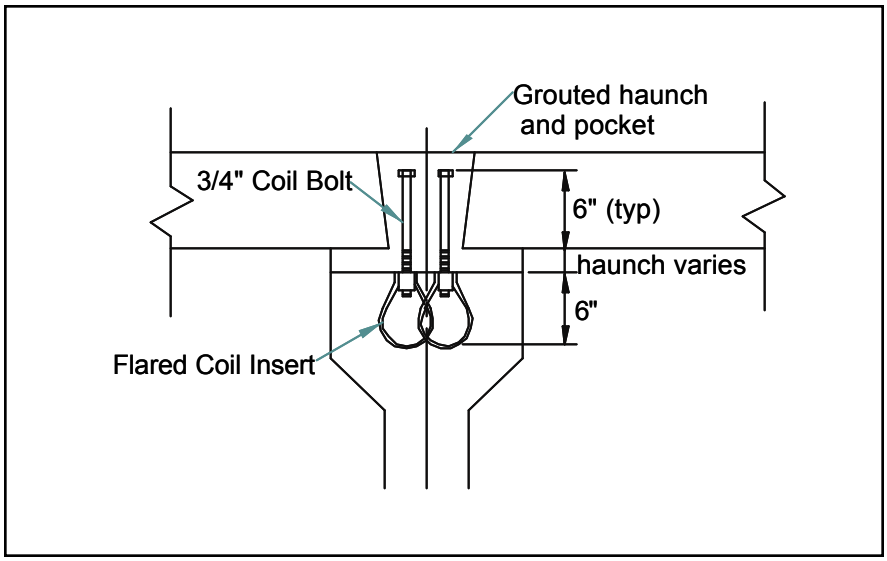

Fig. 14. Dayton-Richmond coil insert.

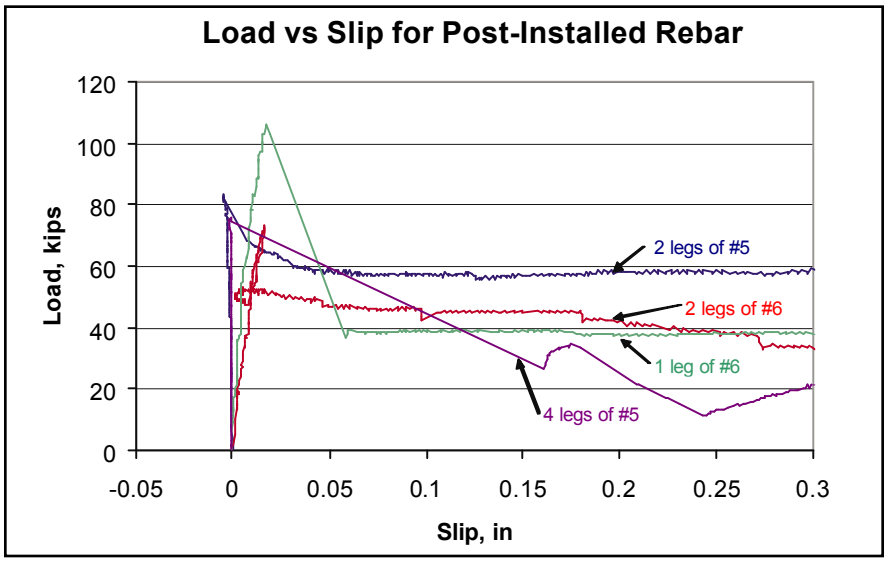

Fig. 15. Load-slip behavior of post-installed reinforcing bars.

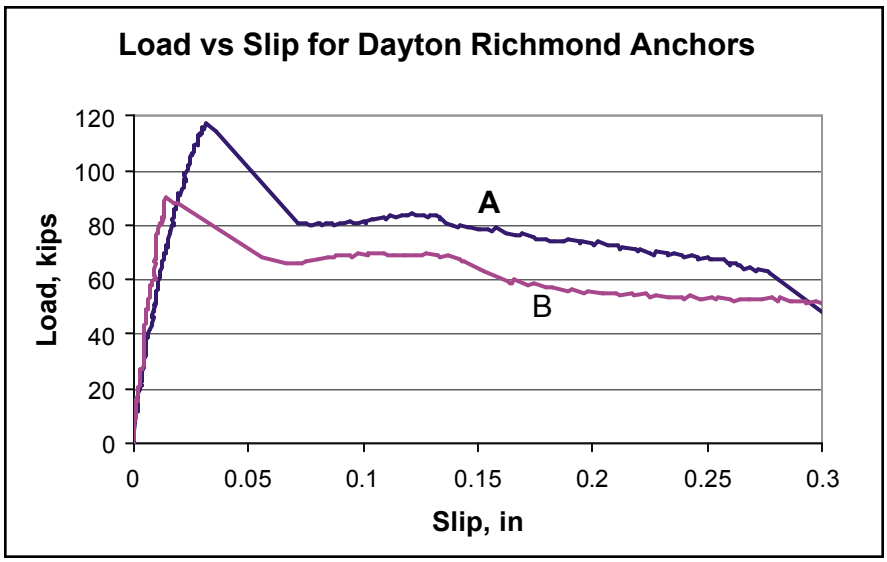

Fig. 16. Load-slip behavior of Dayton-Richmond anchors.

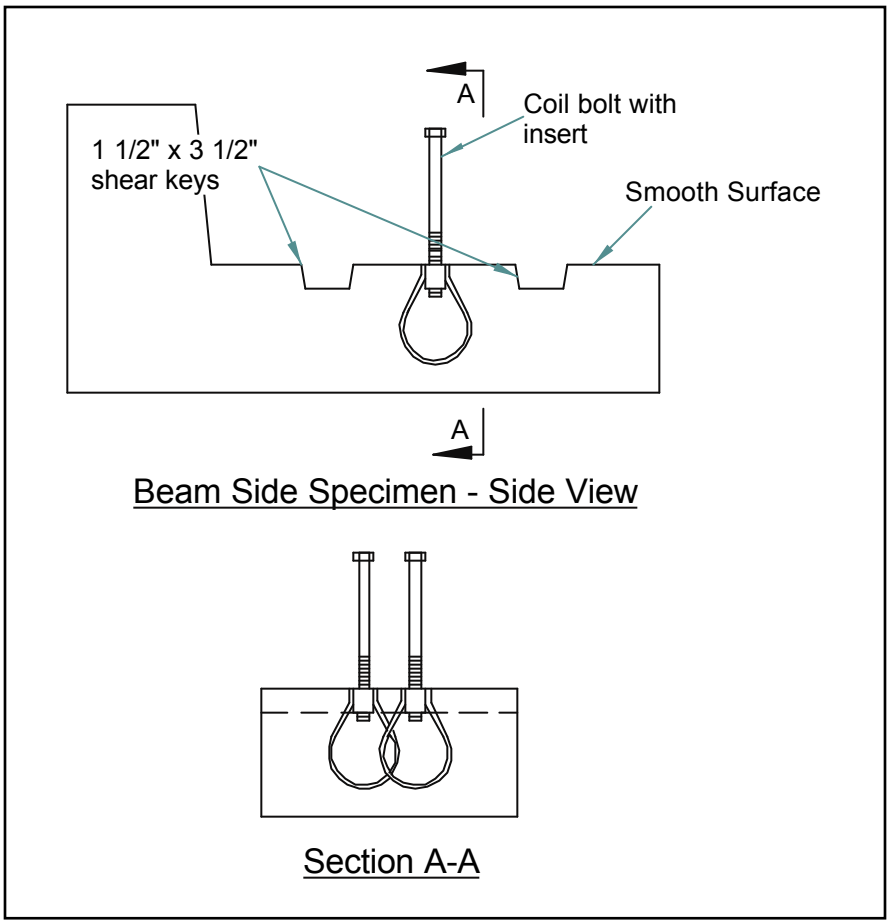

Fig. 17. Specimen with shear keys.

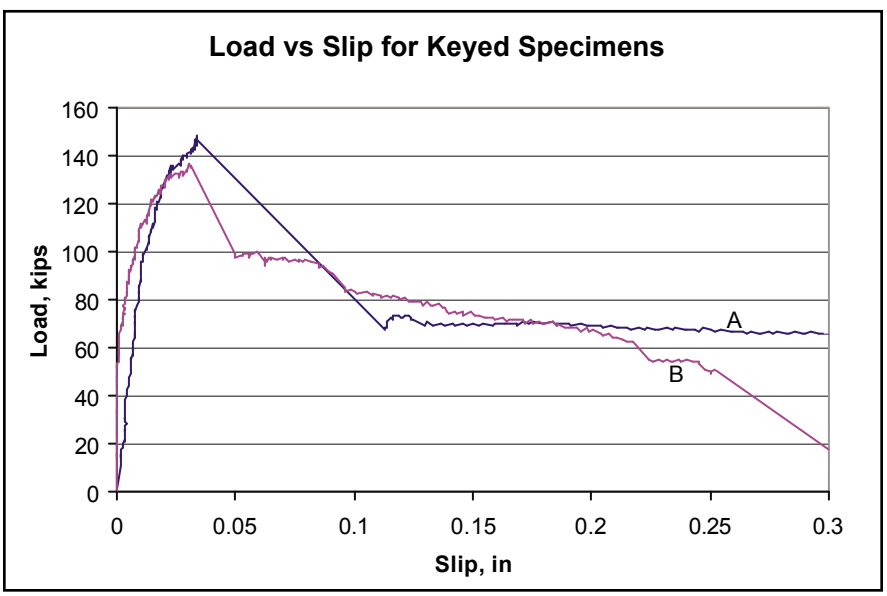

Fig. 18. Load-slip behavior of keyed specimens.

shear keys are illustrated in Fig. 17. This type of system was investigated by Tadros et al.[18] for cast-in-place decks, to create a more easily replaceable deck. To make the deck removal process easier, a debonding agent can be applied to the beam top surface. In this project, however, the debonding agent was not applied.

The load-slip plots for the keyed specimens are presented in Fig. 18. The presence of the shear keys at the top surface of the beam increased the interface peak shear capacity considerably. One of the specimens with shear keys had a maximum capacity of 149 kips (663 kN), and the other specimen had a capacity of 136 kips (605 kN), compared to the maximum capacity with a roughened interface of 130 kips (578 kN). The crack that formed at the peak load formed along the beam-haunch interface and passed through the shear keys. The sustained post-peak load was close to that of similar specimens without shear keys.

Strength Prediction

The results from all 36 push-off tests are presented in Table 4. In addition to the peak load, a post-peak load is also listed. The post-peak load is the average load carried from immediately after cracking to 0.3 in. (8 mm) of slip. The specimens that have no presented post-peak load showed a steadily dropping load over the slip interval.

The results of 34 of the tests were used to develop an equation to quantify the horizontal shear resistance when precast panels are supported on precast girders with a 1 to 3 in. (25 to 76 mm) grouted haunch. Tests 35 and 36 were not included in the derivation of the equation because the contact surface of the beam element was different from the others. The data are presented in Fig. 19 for the peak shear stress versus the clamping stress across the joint.

Two lines, representing equations, are presented in this figure. The upper equation is a best fit of the test data and was derived using the method of least squares. The lower line is a lower-bound equation for the peak shear stress. It was derived by first calculating the difference between the test load and the load predicted with the best fit equation for each specimen.

Then, the standard deviation of the difference for the set of specimens was determined. A value equal to 1.64 times the standard deviation was subtracted from the y-axis intercept of the best fit equation, but the slope was not changed. This equation results in a 95 percent probability that measured strength will exceed the calculated strength.

The best fit equation is:

$$v_{nh} = 160 + 0.51\frac{A_{vh}f_y + P_n}{b_v s} \quad (4)$$

The lower bound equation is:

$$v_{nh} = 80 + 0.51\frac{A_{vh}f_y + P_n}{b_v s} \qquad (5)$$

where v_{nh} is the nominal horizontal shear resistance in terms of stress, in psi units.

Measured Peak Stresses Compared to Design Equations

The test results were compared to equations for calculating horizontal shear resistance in ACI 318-02,[8] the AASHTO Standard Specifications for Highway Bridges,[9] and the AASHTO LRFD Bridge Design Specifications.[10] This comparison is presented in Fig. 20. Note that the clamping stress as defined by ACI 318-02 and the AASHTO Standard Specifications does not include the applied normal force.

The equation presented in the AASHTO LRFD Specifications most accurately predicts test loads from this research. It predicts the strength of 61 percent of the test specimens conservatively. The equations presented in the ACI 318-02 Code and the AASHTO Standard Specifications are generally unconservative for the precast panel system. They are conservative for low amounts of reinforcement crossing the interface and unconservative for larger amounts of reinforcement.

It should be kept in mind that the difference between the test results and the code equations may be attributed to the fact that in this project, both beam and slab elements were precast members and were bonded by means of grouting. The code equations were developed for the case of new concrete cast against old concrete.

Post-Peak Strength

Fig. 21 presents the full data set for post-peak sustained stress versus the clamping stress across the joint. This plot also includes a best fit line derived using the method of least squares.

The best fit equation for post-peak sustained stress is as follows:

$$v_{nh} = 27 + 0.77\frac{A_{vh}f_y + P_n}{b_v s} \qquad (6)$$

This equation represents the load that can be maintained across the open crack through extended slips.

One way to model the post-peak behavior of the push-off tests is through

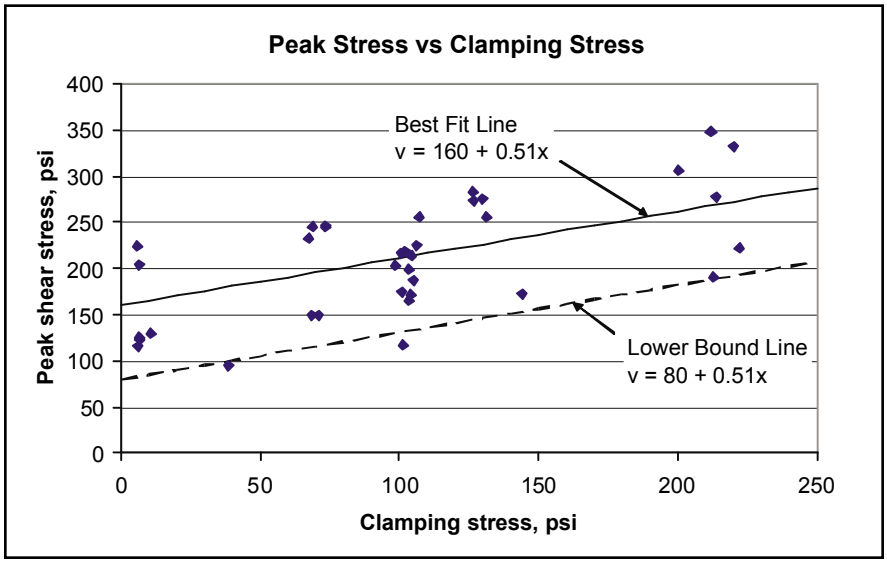

Fig. 19. Peak stress versus clamping stress from all push-off tests and best fit line.

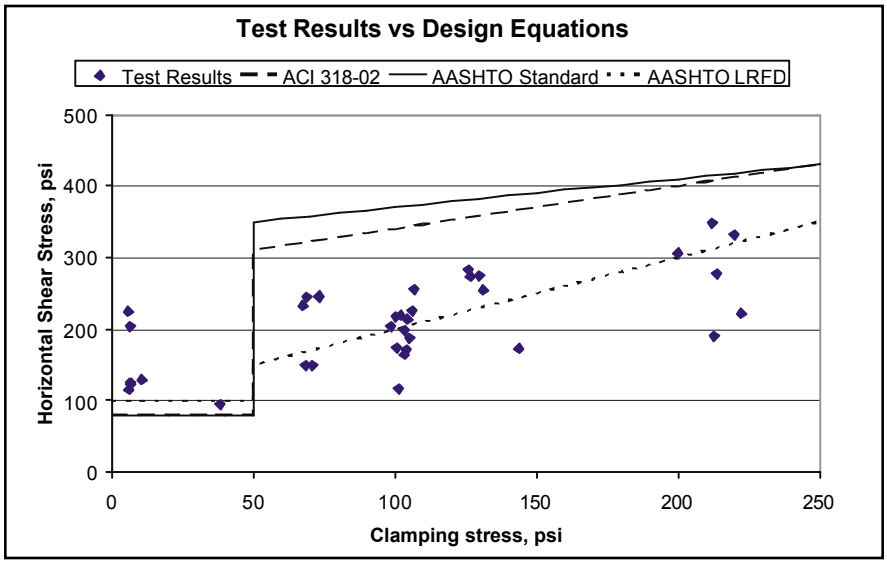

Fig. 20. Peak stresses from push-off tests compared to design equations.

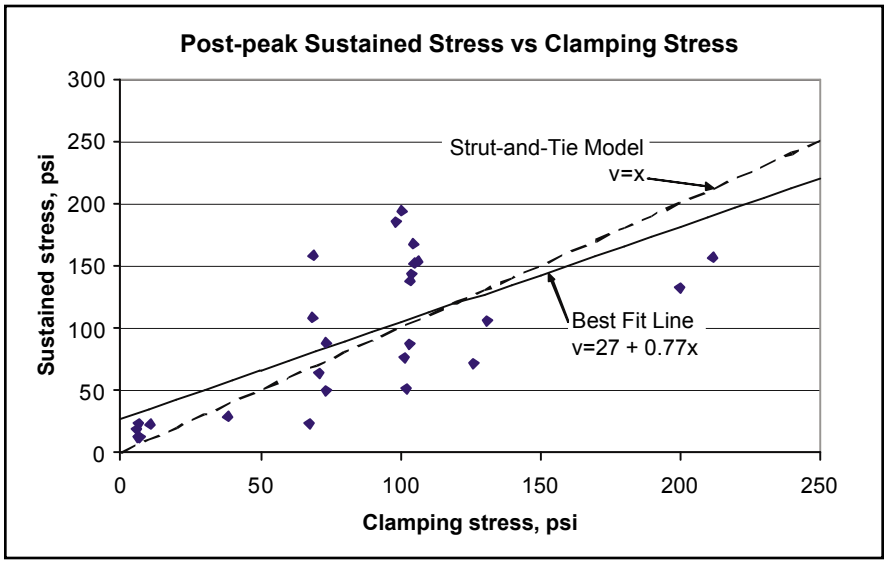

Fig. 21. Post-peak sustained stress versus clamping stress from all push-off tests.

strut-and-tie modeling. The objective of strut-and-tie modeling is to establish a truss, which consists of compression elements (struts) and tension elements (ties), and which represents the flow of forces in the considered region.

Fig. 22 shows a possible strut-and-tie model for the push-off specimens. The dashed lines represent the compression struts and the solid lines the tension ties. By statics, a relationship between the tension tie that represents the shear connectors and the applied force may be established.

Examining the model in Fig. 22, it can be seen that if the maximum tie force $T = A_s f_y$, then the corresponding shear force $P = T\tan\theta$. In the specimens of this test program, depending on the location of Nodes A and B in the model, the angle θ will vary between 40 and 50 degrees. For an average angle of 45 degrees, this would result in a prediction of the shear strength of $A_s f_y$. A line representing this strength is shown in Fig. 21, and compares reasonably well to the post-crack strength of the specimens.

DISCUSSION OF TEST RESULTS

The observed behavior of the specimens brings somewhat into question the applicability of the code horizontal shear equations to the situation represented by the test specimens. The equations are presented as a cohesion value, which also encompasses such factors as dowel action, plus a friction coefficient times the clamping force, typically defined as $A_s f_y$.

The results of this testing program indicate that, in this type of specimen, at the time that the peak stress is attained, there has not been enough relative movement across the interface to result in the yielding of the reinforcement. It is only after the crack forms that the steel yields, and at that time the cohesion is all but lost.

Therefore, for this type of specimen, before cracking, the coefficient on the $A_s f_y$ term is an expression of the effectiveness of the reinforcement present in elevating the cracking load, but to refer to it as a friction coefficient is misleading. In shear planes in monolithic concrete and at the interface between precast and cast-in-place concrete, cracking along the interface occurs progressively and the reinforcement does reach yield at peak load.

One approach to the design of the interfaces of the type considered in this study is for the designer to investigate two possible methods. The first method is to use a low strength reduction factor on the peak strength, because of the high variability of the strengths and the brittle behavior. This design strength would then be compared to the horizontal shear demand at each section along the beam, and should ensure the interface is uncracked.

The second method is to use a higher strength reduction factor with the post-crack strength, to acknowledge the ability of the connection to maintain load through extended slips, and thereby allow redistribution of the forces among adjacent connectors. The summation of the strength of all the connectors between the support and point of maximum moment would be compared against the total change in the compressive force in the deck between the two points, which would ensure full composite action.

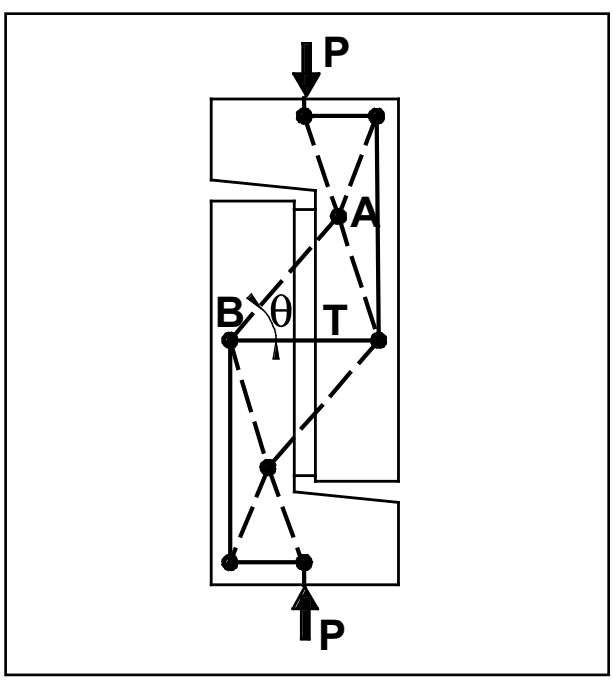

Fig. 22. Strut-and-tie model of push-off tests.

CONCLUSIONS AND RECOMMENDATIONS

This paper has presented the results of a test program to investigate the horizontal shear strength of the connection between a precast concrete girder and a precast concrete deck panel. Primary conclusions from this research are as follows:

1. The Set 45 formulation developed slightly higher peak shear stresses than the latex modified grout.

2. There was no significant difference in peak shear stress between specimens with 1, 2, and 3 in. (25, 51, and 76 mm) haunch heights.

3. The extended stirrups must be detailed to have a minimum of 5 in. (127 mm) embedment into the deck panel.

4. The alternate shear connectors investigated in this study are viable for use with the precast panel system.

5. In addition, equations have been presented to quantify the shear stress to cause cracking at the interface between the two elements and to quantify the stress that can be carried across the cracked interface. Among the current codes and specifications, the equation in the AASHTO LRFD Specifications is the best predictor of the peak interface strength.

6. Designers of this type of clustered connection must prevent a cone breakout type of failure that may occur if many connectors are clustered together in one location or if the embedment is inadequate. Proper embedment and spacing of connectors will ensure yielding of the steel and ductile behavior of the interface.

ACKNOWLEDGMENTS

This research was performed at the Structures and Materials Laboratory at Virginia Tech. The work was funded by the Precast/Prestressed Concrete Institute through a Daniel P. Jenny Fellowship, the Virginia Center for Innovative Technology, and Bayshore Concrete Products. This support is gratefully acknowledged. In addition, the guidance and support provided by Vincent Campbell of Bayshore Concrete Products is greatly appreciated.

The authors also want to express their appreciation to the PCI JOURNAL reviewers for their constructive comments.

The opinions presented herein are those of the researchers and not necessarily of the sponsors.

REFERENCES

1. Issa, M. A., Yousif, A. A., and Issa, M. A., "Construction Procedures for Rapid Replacement of Bridge Decks," *Concrete International*, V. 17, No. 2, February 1995, pp. 49-52.
2. Issa, M. A., Yousif, A. A., Issa, M. A., Kaspar, I. I., and Khayyat, S. Y., "Analysis of Full Depth Precast Concrete Bridge Deck Panels," PCI JOURNAL, V. 43, No. 1, January-February 1998, pp. 74-85.
3. Issa, M. A., Idriss, A. T., Kaspar, I. I., and Khayyat, S. Y., "Full Depth Precast and Precast, Prestressed Concrete Bridge Deck Panels," PCI JOURNAL, V. 40, No. 1, January-February 1995, pp. 59-80.
4. Issa, M. A., Yousif, A. A., Issa, M. A., Kaspar, I. I., and Khayyat, S. Y., "Field Performance of Full Depth Precast Concrete Panels in Bridge Deck Reconstruction," PCI JOURNAL, V. 40, No. 3, May-June 1995, pp. 82-107.
5. Yamane, T., Tadros, M. K., Badie, S. S., and Baishya, M. C., "Full-Depth Precast Prestressed Concrete Bridge Deck System," PCI JOURNAL, V. 43, No. 3, May-June 1998, pp. 50-66.
6. Chang, P. S., and Shim, S. S., "Continuous Composite Bridges with Precast Decks," *Steel Structures,* September 2001, pp. 123-132.
7. Shim, C. S., Kim, J. H., Chang, S. P., and Chung, C. H., "The Behavior of Shear Connections in a Composite Beam with a Full Depth Precast Slab," *Structures and Buildings,* Proceedings of the Institution of Civil Engineers, February 2000, pp. 101-110.
8. ACI Committee 318, "Building Code Requirements for Structural Concrete (ACI 318-02)," American Concrete Institute, Farmington Hills, MI, 2002.
9. AASHTO, *Standard Specifications for Highway Bridges,* Sixteenth Edition, American Association of State Highway and Transportation Officials, Washington, DC, 1996.
10. AASHTO, *LRFD Bridge Design Specifications,* Second Edition, American Association of State Highway and Transportation Officials, 1998, with 1999, 2000, 2001 and 2002 Interims, Washington, DC, 1998.
11. Mast, R. F., "Auxiliary Reinforcement in Concrete Connections," *ASCE Journal*, V. 94, No. ST6, June 1968, pp. 1485-1504.
12. Mattock, A. H., "Shear Transfer in Reinforced Concrete," *ACI Journal*, V. 69, No. 2, February 1969, pp. 17-42.
13. Mattock, A. H., and Hawkins, M. N., "Shear Transfer in Reinforced Concrete—Recent Research," PCI JOURNAL, V. 17, No. 2, March-April 1972, pp. 55-75.
14. Mattock, A. H., " Shear Transfer in Concrete Having Reinforcement at an Angle to the Shear Plane," *Shear in Reinforced Concrete*, SP-42, V. 1, American Concrete Institute, Detroit, MI, 1974, pp. 17-42.
15. Mattock, A. H., Li, W. K., and Wang, T. C., "Shear Transfer in Lightweight Reinforced Concrete," PCI JOURNAL, V. 21, No. 1, January-February 1976, pp. 20-39.
16. Birkeland, P. W., "Connections in Precast Concrete Construction," *ACI Journal*, V. 63, No. 3, March 1966, pp. 345-367.
17. Menkulasi, F., "Horizontal Shear Connectors for Precast Prestressed Bridge Deck Panels," Master's Thesis, Department of Civil and Environmental Engineering, Virginia Polytechnic Institute and State University, Blacksburg, VA, 2002.
18. Tadros, K. M., Badie, S. S., and Kamel, R. M., "Girder Deck Connection for Rapid Removal of Bridge Decks," PCI JOURNAL, V. 47, No. 3, May-June 2002, pp. 58-69.

APPENDIX A – NOTATION

A_{vh} = area of horizontal shear reinforcement, sq in.
b_v = width of top flange, in.
C = cohesion
d = depth to tension reinforcing or prestressing steel, in.
f'_c = nominal concrete compressive strength, psi
f_y = yield strength of reinforcing steel, psi
P_c = permanent compressive force across interface, lbs
P_n = normal force across joint, lbs
s = spacing of horizontal shear reinforcement, in.
v_{nh} = nominal horizontal shear resistance in terms of stress, psi
V_{nh} = nominal horizontal shear strength, lbs
V_{max} = maximum applied shear force, lbs
V_{peak} = peak shear load, lbs
v_{peak} = peak shear stress, psi
v_{clamp} = clamping stress, psi
V_{sust} = sustained shear load, lbs
v_{sust} = sustained shear stress, psi
v_{uh} = factored horizontal shear stress, psi
V_u = factored vertical shear force, lbs
μ = friction coefficient
ϕ = strength reduction factor